Supplementary Material:

Gli2 regulates cell-cycle progression in kidney fibrosis and is a novel therapeutic target

Rafael Kramann, Susanne V. Fleig, Rebekka K. Schneider, Steven L. Fabian, Derek P. DiRocco, Omar Maarouf, Janewit Wongboonsin, Yoichiro Ikeda, Dirk Heckl, Steven L. Chang, Helmut G. Rennke, Sushrut S. Waikar and Benjamin D. Humphreys

Address to correspond to:
Benjamin D Humphreys, MD, PhD
Renal Division, Department of Medicine, Washington University School of Medicine;
Box 8126, 600 South Euclid Avenue, St. Louis, Missouri 63110
E-mail: bhumphre@dom.wustl.edu

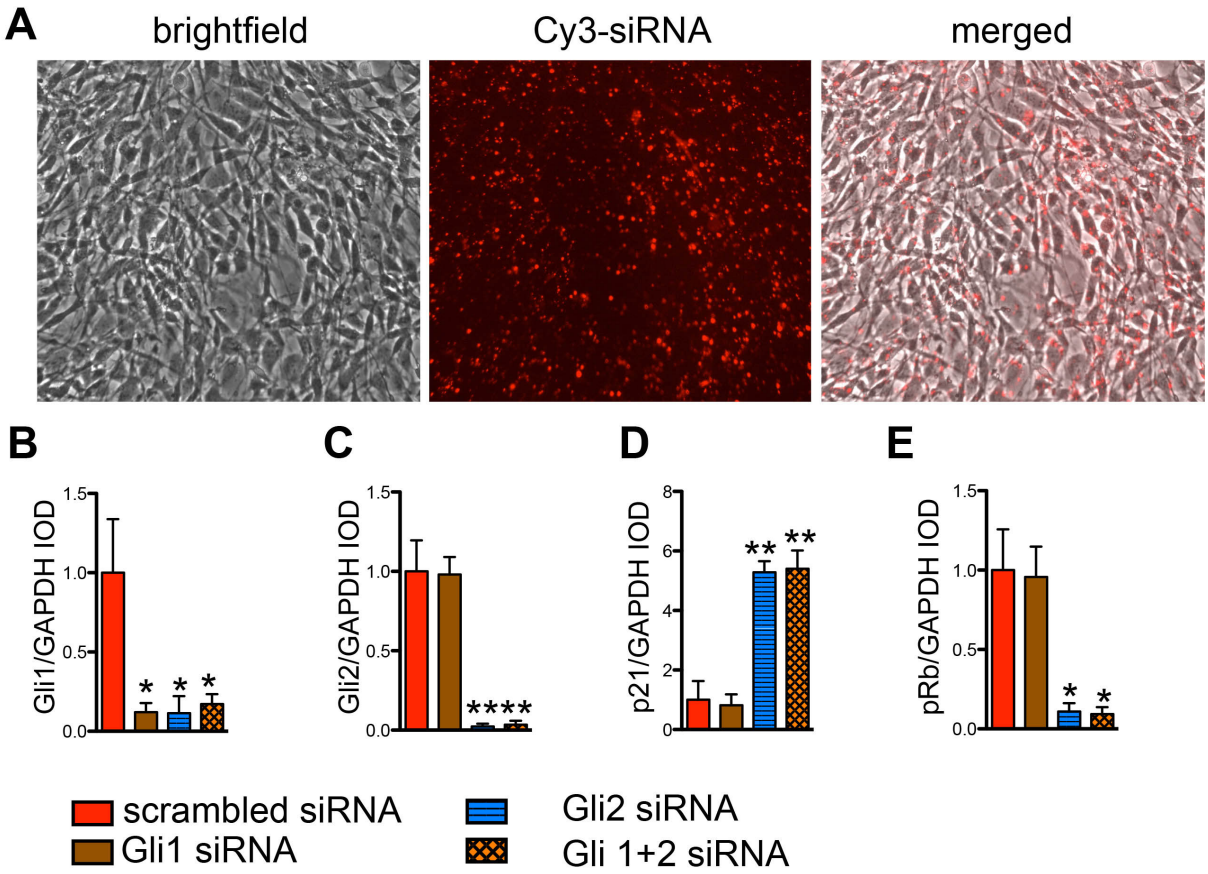

Figure S1: SiRNA knockdown of Gli2 induces p21 expression with reduced phosphorylation of retinoblastoma.

A: To monitor the efficiency of siRNA delivery to 10T1/2 cells we used a fluorochrome (Cy3) labeled siRNA against GAPDH. Pictures were taken after washing the cells with phosphate buffered saline indicating a successful and high efficient transfection.

B-E: Western blots from 2 experiments (total of n=3 biological replicates) of siRNA mediated knockdown of Gli1, Gli2 or Gli1+2 were quantified by integrated optical density (IOD). *p<0.05; **p<0.01 by one way ANOVA with posthoc Bonferroni , data presented as mean±SEM.

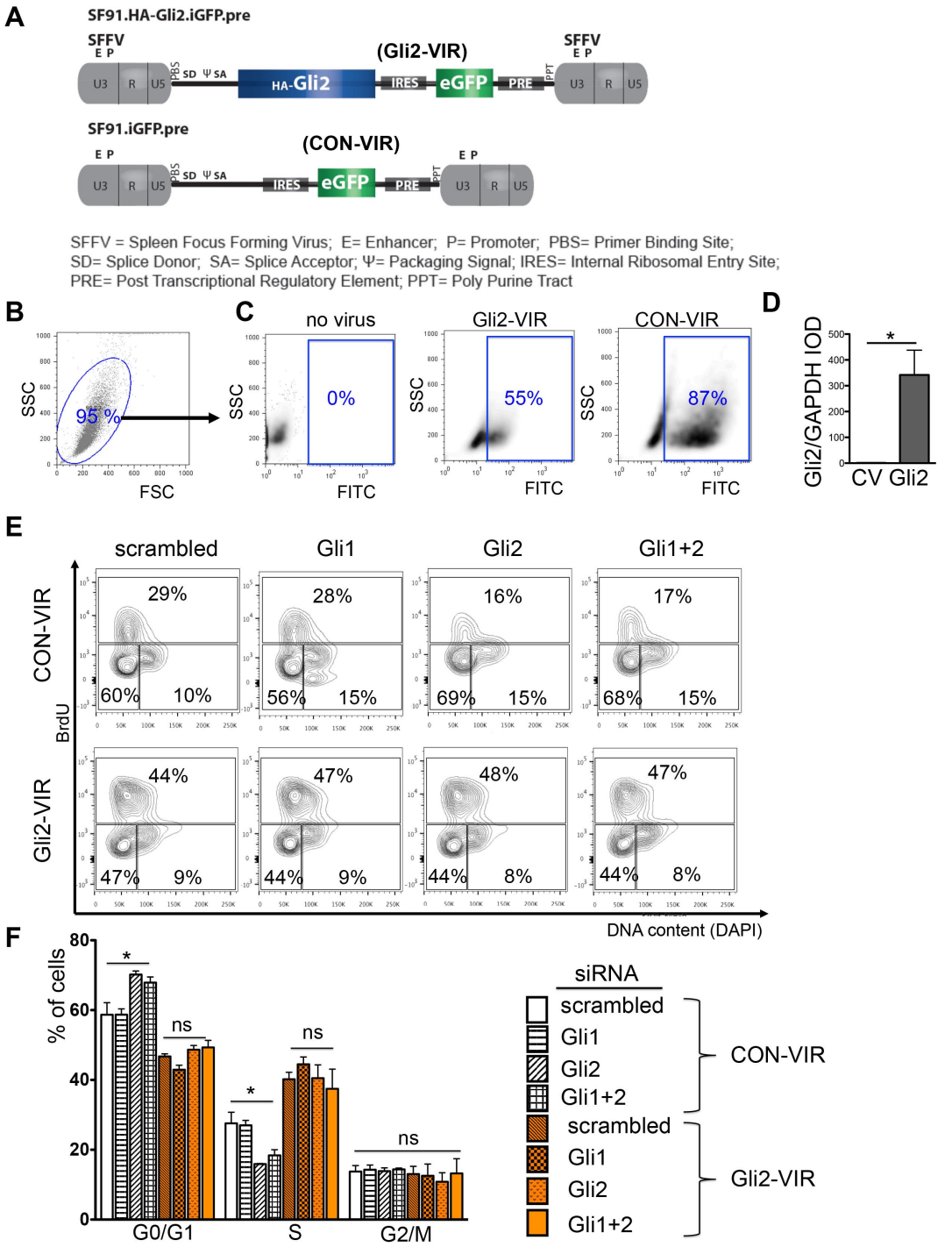

Figure S2: Gli2 overexpression induces proliferation and rescues the effect of siRNA knockdown

A: Scheme of the retrovirus used for overexpression of Gli2 (SF91.HA-Gli2.iGFP.pre) and the control virus (SF91.iGFP.pre).

B-C: After initial gating of a population regarding forward and sideward scatter of the cells (FSC, SSC) (B) only the GFP expressing cells were included into further cell-cycle analysis (C).

D: Western blots of 10T1/2 cells transduced with the Gli2 retrovirus (Gli2) and the control virus (CV) were quantified by integrated optical density (IOD) (data of 2 experiments with a total of n=4 biological replicates).

E: Representative flow cytometric plots for cell-cycle analysis of 10T1/2 cells treated with siRNA against Gli1, Gli2, Gli1 and Gli2 or control (scrambled) with addition of a Gli2 expressing retrovirus (Gli2-VIR) versus a control virus (CON-VIR).

F: Quantification of cell-cycle flow cytometry demonstrates a G0/G1 cell-cycle arrest in the control virus treated cells after knockout of Gli2 or Gli1 and Gli2 whereas overexpression of Gli2 (Gli2-VIR) increased proliferation and was able to rescue this effect of Gli2 siRNA.

*p<0.05 by T-Test in D, by two way ANOVA with posthoc Bonferroni in F, data presented as mean±SEM.

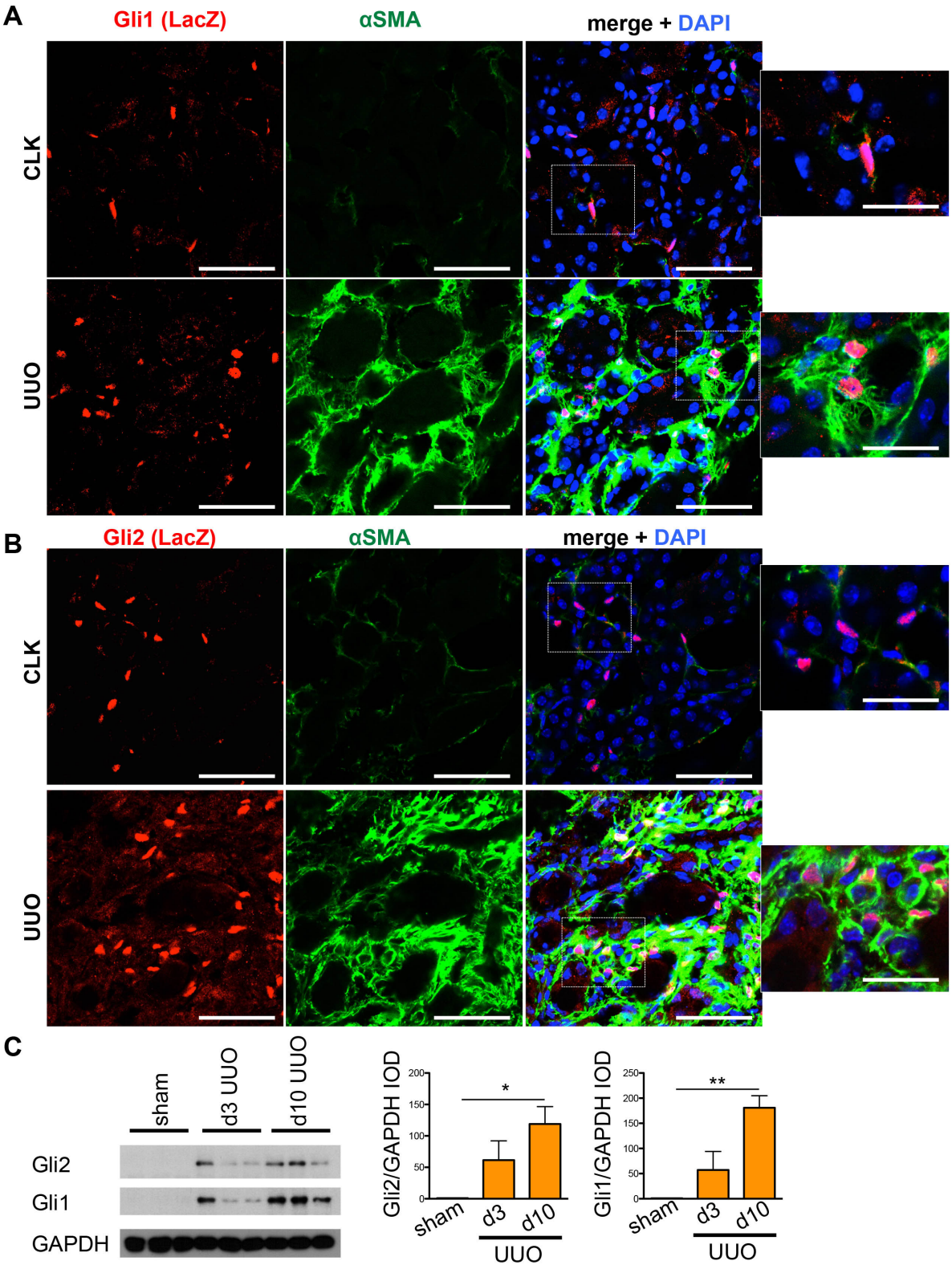

Figure S3: Increased expression of Gli1 and Gli2 in kidney fibrosis specifically expressed in interstitial myofibroblasts.

A-B: Representative images of day 10 UUO kidneys Gli1-nLacZ and Gli2-nLacZ mice (8-10 week of age, both transgenic lines are on a mixed background of 129S, Swiss Webster and C57Bl/6J) costained for β-galactosidase (LacZ) and alpha smooth muscle actin (α-SMA).

C: Representative western blots and quantification by integrated optical density (IOD) for Gli1 and Gli2 expression in wiltype mice (C57Bl/6J, all males 8-10 week of age) subjected to UUO (day 3 and day 10) or sham surgery (n=3 each). *p<0.05, **p<0.01 by one way ANOVA with posthoc Bonferroni. All scale bars 50μm, inserts 25μm.

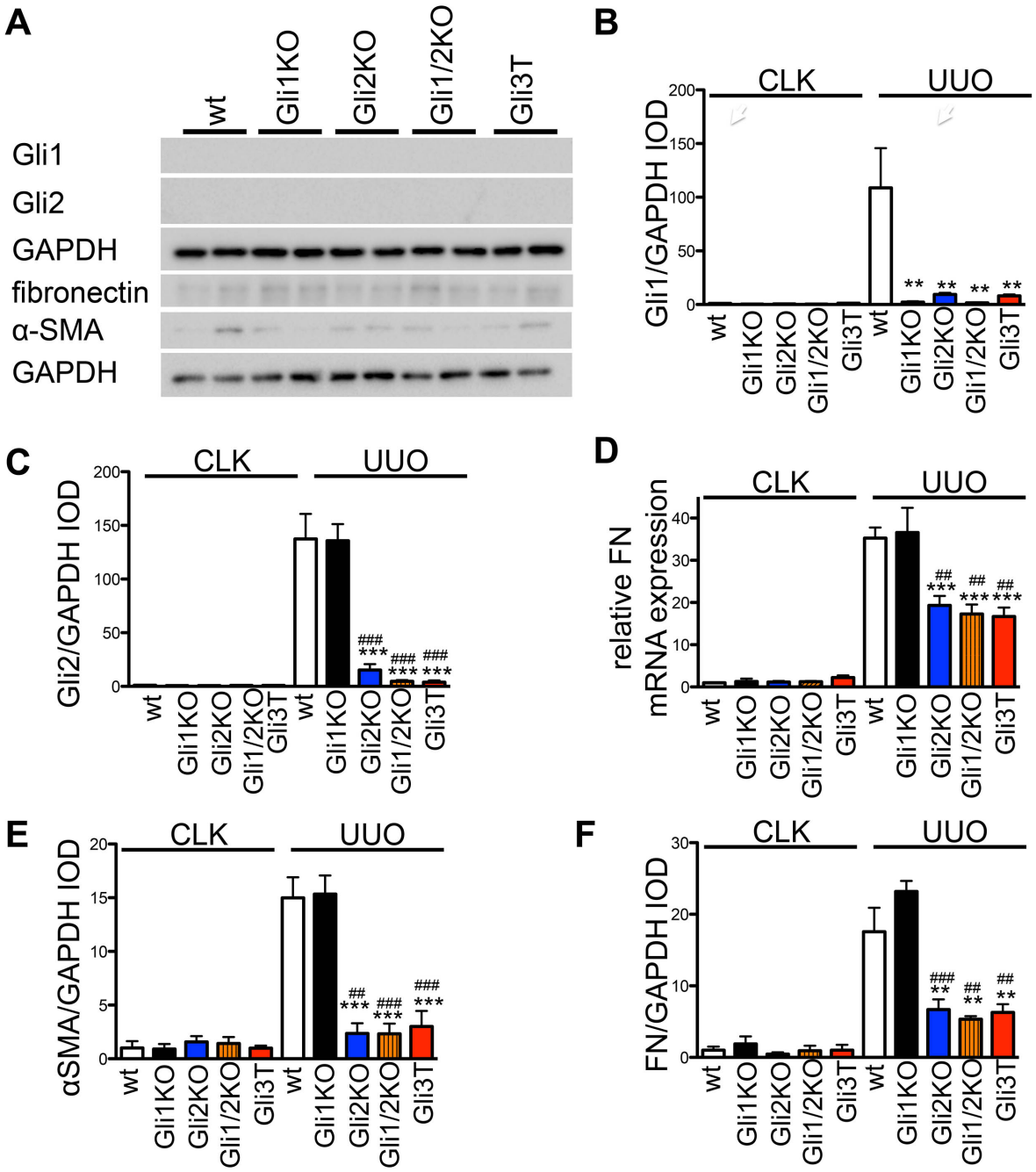

Figure S4: Reduced fibrosis severity following UUO in conditional knockout of Gli1 or Gli3 repressor expression in Gli1^{+} cells

A: Representative western blots of contralateral kidneys (CLK) from wildtype littermates (wt) compared to Gli1KO (Gli1CreER$^{t2+/+}$;Gli2flox$^{-/-}$); Gli2KO (Gli1CreER$^{t2+/-}$;Gli2flox$^{+/+}$); Gli1/2KO (Gli1CreER$^{t2+/+}$;Gli2flox$^{+/+}$) and Gli3T (Gli1CreER$^{t2+/-}$;Gli3T$^{+/-}$) mice. Note: Gli proteins were not detectable in CLK kidneys. All used transgenic mice underwent surgery at 8-10 weeks of age and can be considered as mixed background with C57Bl/6J and 129S. Wildtype controls were littermates of the transgenic mice used in the experiments.

B-E: Protein levels from whole kidney lysates of CLK or unilateral ureteral obstruction (UUO) kidneys of n=4 mice from each group were quantified by integrated optical density -IOD Gli1, Gli2, fibronectin (FN) or αSMA /IOD glyceraldehyde-3-phosphate dehydrogenase (GAPDH).

F: Fibronectin mRNA expression in whole UUO and contralateral kidneys (CLK) of Gli1KO, Gli2KO, Gli1/2KO, Gli3T mice and wiltype littermates (wt). **p<0.05, ***p<0.001 versus wt, , ##p<0.01, ###p<0.001 versus Gli1KO, by one way ANOVA with posthoc Bonferroni , data presented as mean±SEM.

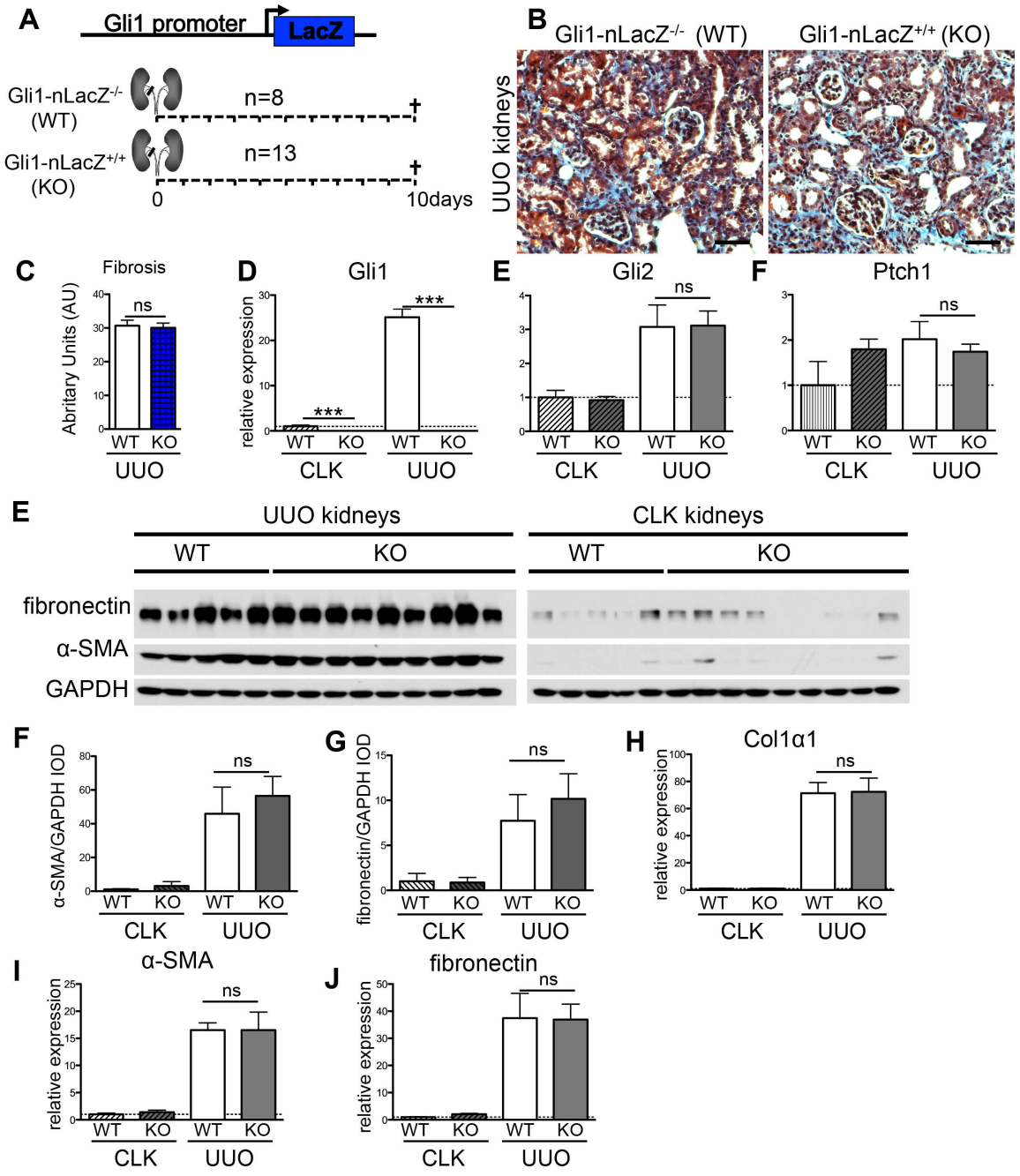

Figure S5: Knockout of the hedgehog effector Gli1 does not reduce renal fibrosis in unilateral ureteral obstruction (UUO)

A: Gli1 knockout (KO) was achieved by generating homozygous Gli1-nLacZ$^{+/+}$ mice (mixed background of 129S, Swiss Webster and C57Bl/6J) as their β-galactosidase knock-in mutation abolishes the Gli1 gene function. Gli1$^{+/+}$(KO) mice n=13 (all males, 8-10 weeks old) and their Gli1$^{-/-}$ wiltype (WT) littermates (n=8, all males, 8-10 weeks old) were subjected to UUO surgery and sacrificed at day 10 after surgery (A).

B-C: Knockout of Gli1 does not alter the extent of interstitial fibrosis. Trichrome stained kidney sections (B) were blindly scored for the extent of interstitial fibrosis (C)

D: Gli1 knockout abolishes the expression of Gli1 in UUO and contralateral control kidney (CLK), whereas the increased expression of Gli2 and Ptch1 in UUO was not effected. **E-G:** The increased expression of fibrotic readouts alpha smooth muscle actin (α-SMA) and fibronectin in UUO compared to CLK was not effected on protein level by knockout of Gli1 (Gli1$^{+/+}$; KO) compared to wildtype (Gli1$^{-/-}$; WT) littermates, as determined by Western blot (E) and quantified by integrated optical density (IOD) (F, G) IOD (α-SMA or IOD fibronectin/IOD glyceraldehydes-3-phosphate dehydrogenase (GAPDH)).

H-J: Quantification of mRNA expression by quantitative realtime PCR does not reveal a significant effect of Gli1 knockout (KO) on expression of increased fibrotic readouts collagen-1-alpha-1 (Col1α1, H), alpha smooth muscle actin (α-SMA, I) or fibronectin (J) in UUO kidneys compared to wildtype (WT) littermates. ns-non signficiant, ***p<0.001 by t-test, data is presented as mean±SD, scale bars 50µm.

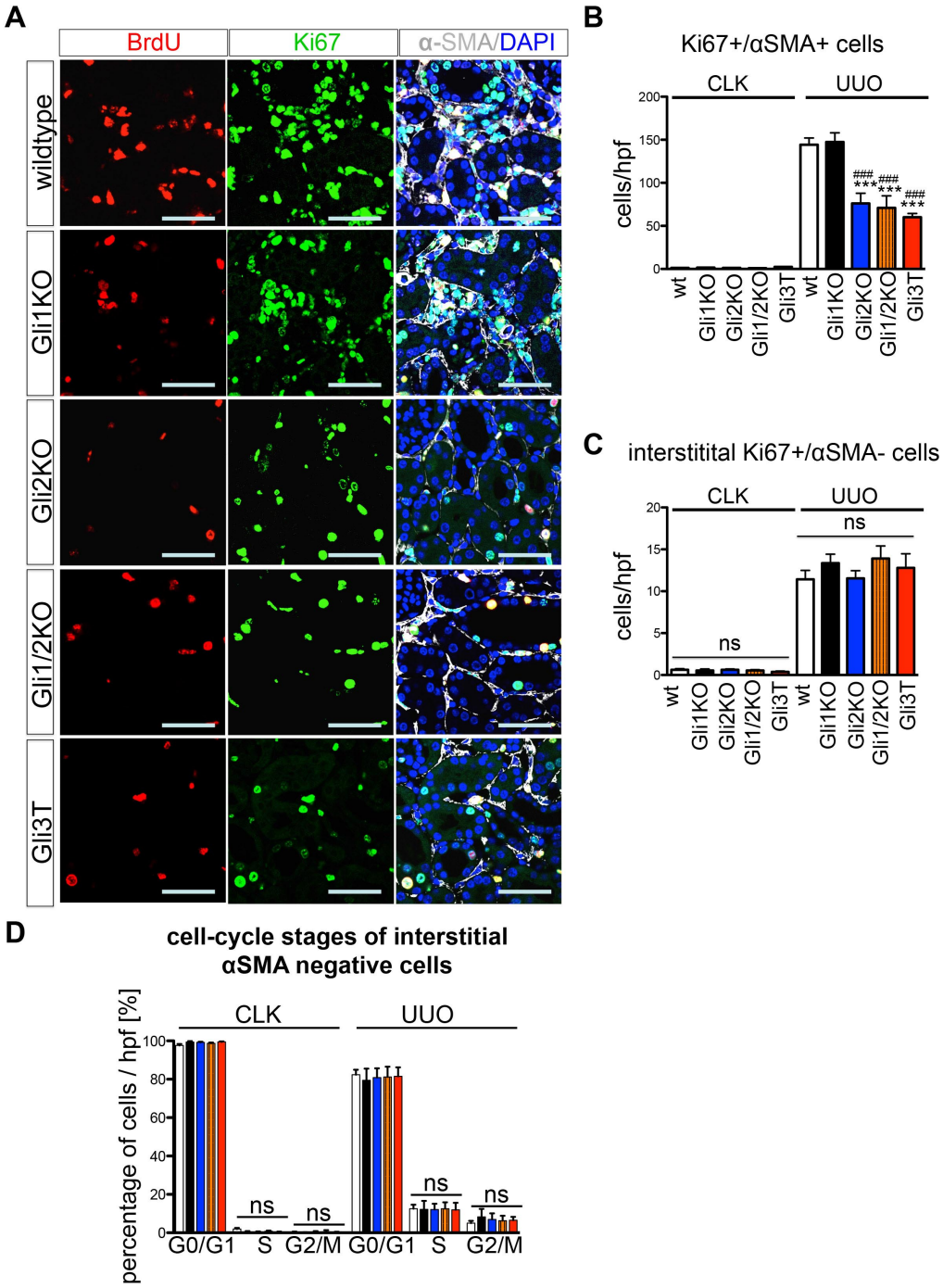

Figure S6: Conditional knockout of Gli2 or expression of the Gli3 repressor reduces proliferation of renal myofibroblasts.

A: Representative pictures of day 10 unilateral ureteral obstruction (UUO) kidneys from wildtype littermates (wt) compared to Gli1KO ($Gli1CreER^{t2+/+}$;$Gli2flox^{-/-}$); Gli2KO ($Gli1CreER^{t2+/-}$;$Gli2flox^{+/+}$); Gli1/2KO ($Gli1CreER^{t2+/+}$;$Gli2flox^{+/+}$) and Gli3T ($Gli1CreER^{t2+/-}$;$Gli3T^{+/-}$) mice co-stained for BrdU, Ki67 and alpha-smooth muscle actin (αSMA). BrdU was given 3 hours before euthanasia. All used transgenic mice underwent surgery at 8-10 weeks of age and can be considered as mixed background with C57Bl/6J and 129S. Wildtype controls were littermates of the transgenic mice used in the experiments.

B: Quantification of cycling (Ki67+) interstitial myofibroblasts (αSMA+) in day 10 UUO and contralateral non-injured kidneys (CLK).

C: Quantification of cycling interstitial non-myofibroblast cells (αSMA-).

D: Cell cycle stages for interstial non-myofibroblast cells (αSMA-) were assessed by counting of all interstitial cells in high power fields (400x) that were negative for αSMA staining after costaining for BrDU (S-phase), phospho-Histone H3 (G2/M-phase; G0/G1-phase: all interstitial $αSMA^-$ cells - interstitial $αSMA^-$ $BrDU^+$ cells - interstitial $αSMA^-/pH3^+$ cells). ***p<0.001 versus wt, ###p<0.001 versus Gli1KO, by one way ANOVA with posthoc Bonferroni , data presented as mean±SEM. Scale bars 50µm.

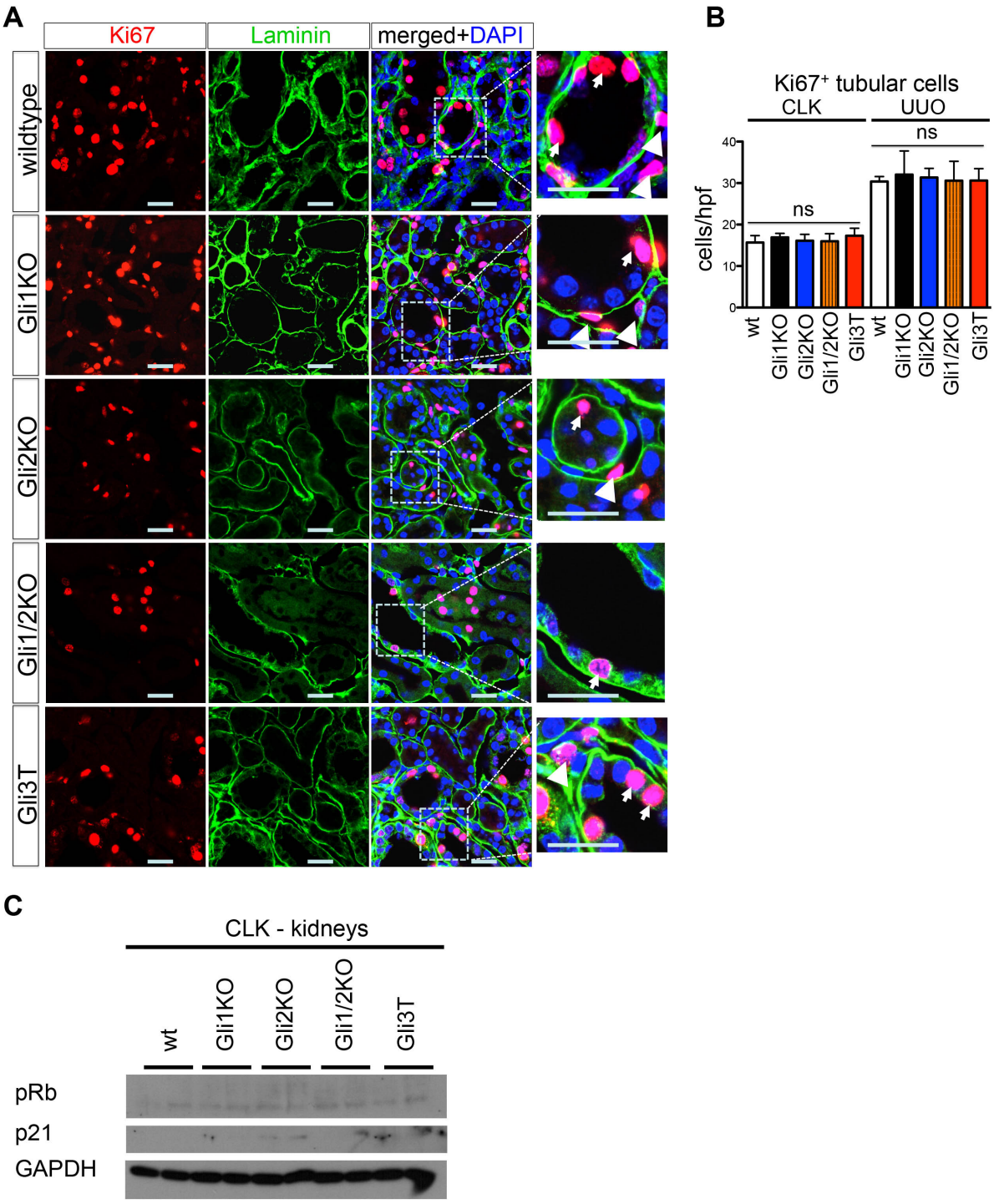

Figure S7: Proliferation of kidney tubular cells is not affected in the conditional knockout experiments.
A: Representative pictures of day 10 unilateral ureteral obstruction (UUO) kidneys from wildtype littermates (wt) compared to Gli1KO (Gli1CreER$^{t2+/+}$;Gli2flox$^{-/-}$); Gli2KO (Gli1CreER$^{t2+/-}$;Gli2flox$^{+/+}$); Gli1/2KO (Gli1CreER$^{t2+/+}$;Gli2flox$^{+/+}$) and Gli3T (Gli1CreER$^{t2+/-}$;Gli3T$^{+/-}$) mice co-stained for Ki67 and laminin to delineate tubular epithelial proliferation. Tubular epithelial cells (arrows) were easily detected as cells within the tubule surrounded by the laminin^{+} basement membrane. Whereas interstitial cells (arrowheads) were located in between two laminin^{+} layers of the basement membrane surrounding neighboring tubules. All used transgenic mice underwent surgery at 8-10 weeks of age and can be considered as mixed background with C57Bl/6J and 129S. Wildtype controls were littermates of the transgenic mice used in the experiments.
B: Tubular epithelial cells positive for the proliferation marker Ki67 were counted in 400x images (7 images / kidney in n=5 mice per group).
C: Representative western blots for phosphorylated retinoblastoma (pRb) and p21 in contralateral kidneys of Gli1KO, Gli2KO, Gli1/2KO, Gli3T mice and wiltype (wt) littermates. ns = non significant by one way ANOVA with posthoc Bonferroni , data presented as mean±SEM. Scale bars 25µm.

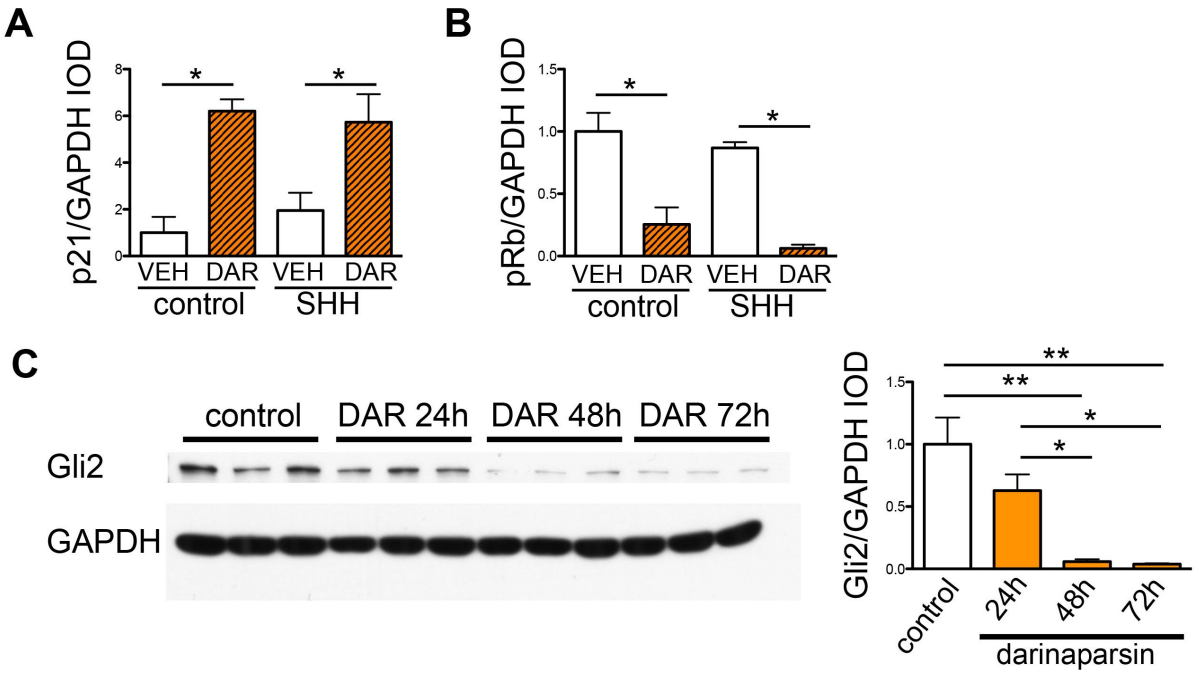

Figure S8: Darinaparsin treatment decreases Gli2 protein levels over time with upregulation of p21 and reduced phosphorylation of retinoblastoma.

A-B: Western blots from 2 experiments (total of n=3 biological replicates) of 10T1/2 cells treated with darinaparsin (DAR) or vehicle (VEH) with addition of sonic hedgehog (SHH) preconditioned medium (or control medium) were quantified by integrated optical density (IOD).

C: Representative western blot and quantification by integrated optical density (IOD) of human embryonic kidney cells (HEK293T) transfected with full-length Gli2 (pcDNA3.1-His-Gli2) and addition of normal saline (control) or darinaparsin (DAR, 0.5µM) over a time-course from 24 to 72 hours.

*p<0.05, **p<0.01, ***p<0.001, by t-test in A,B; by one way ANOVA with posthoc Bonferroni in C, data presented as mean±SEM.

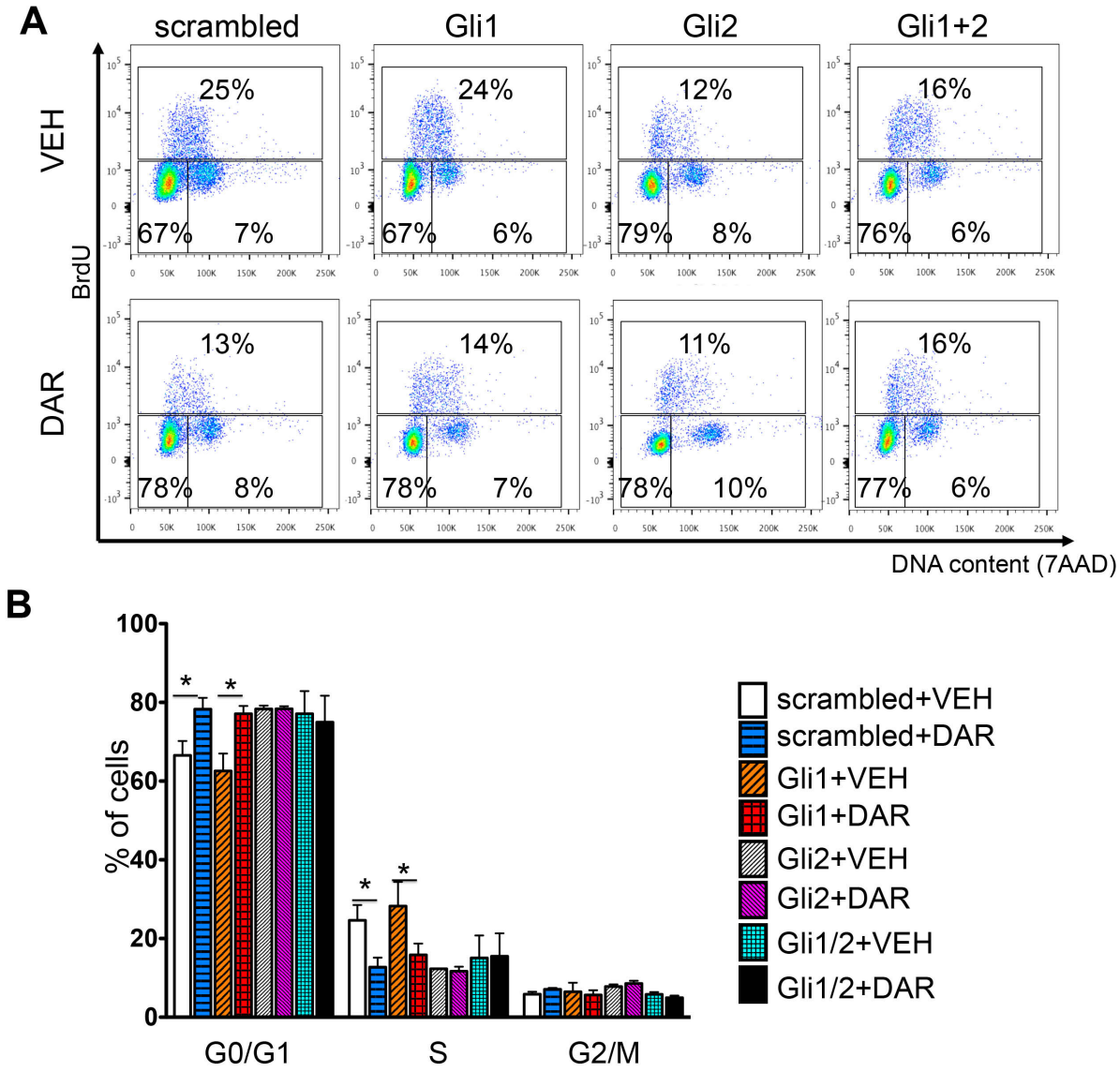

Figure S9: RNAi mediated knockdown of Gli2 abolishes the cell-cycle effect of darinaparsin.
A-B: Representative flow cytometric plots and quantification of 10T1/2 cells treated with siRNA against Gli1, Gli2, Gli1 and Gli2 or scrambled siRNA (control) with addition of darinaparsin (DAR, 0.5µM) or vehicle (VEH, normal saline). Note, darinaparsin treatment resulted in a G0/G1 cell cycle arrest of 10T1/2 cells treated with control siRNA and siRNA against Gli1 whereas siRNA against Gli2 or both Gli1+Gli2 decreased proliferation of cells with no further effect of darinaparsin treatment.
*$p<0.05$, by two way ANOVA with posthoc Bonferroni, data presented as mean±SEM.

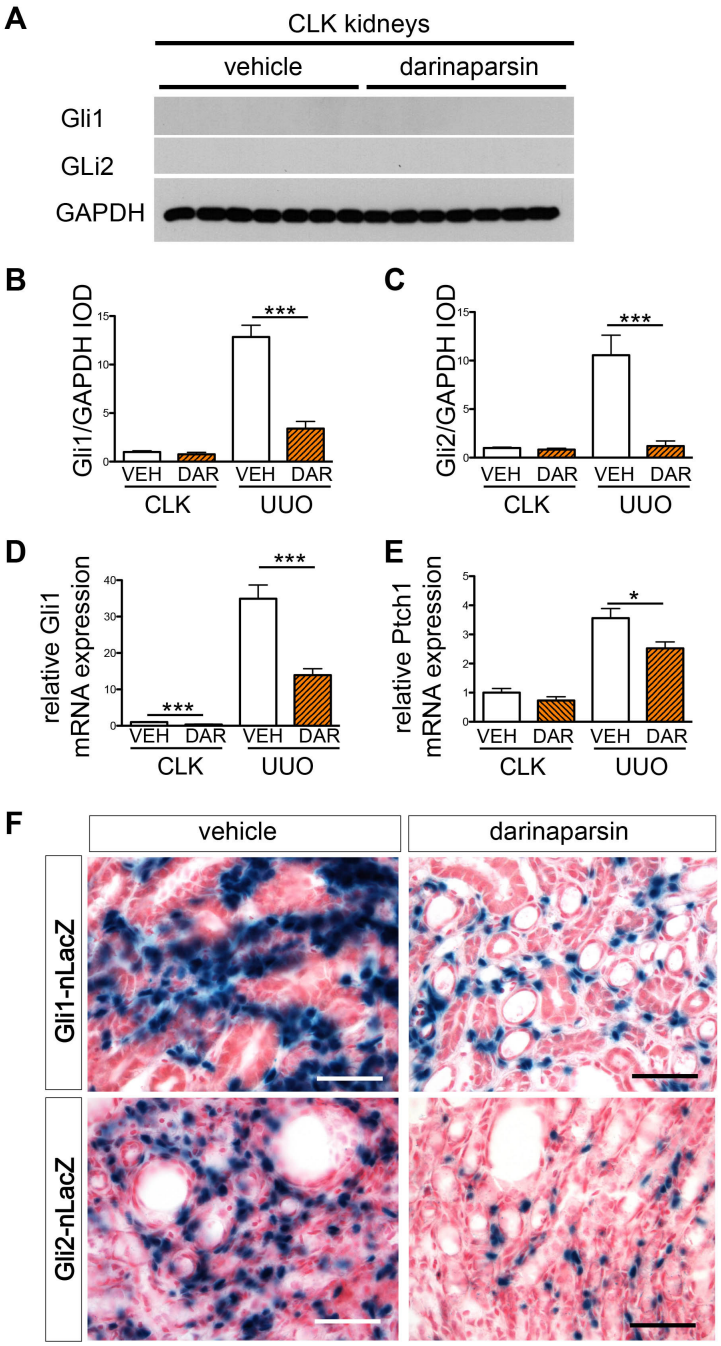

Figure S10: Darinaparsin treatment reduces the number of Gli1 and Gli2 expressing cells following UUO with decreased Gli1 and Gli2 protein levels and reduced hedgehog pathway activity

A: Representative western blots of contralateral (CLK) kidneys from wildtype (C57Bl/6J, 8-10 weeks old, all males) mice treated with darinaparsin (n=7) or vehicle (n=7) starting 2 days prior to UUO surgery until day 10 (blots from UUO kidneys in figure 5B).

B-C: Quantification of Gli1 and Gli2 protein levels in whole kidney lysates (UUO and CLK) of wiltype mice (C57Bl/6J) treated with darinaparsin (DAR, n=7) or vehicle (VEH, n=7) from 2 days prior to UUO surgery until day 10 (Experiment Figure 5 A-G).

D-E: Quantitative realtime PCR from whole kidney lysates of wildtype mice (C57Bl/6J) subjected to UUO (10days) and treated with darinaparsin (DAR, n=9) or vehicle (VEH, n=7) from 2 days prior to UUO surgery until day 10 indicates reduced mRNA expression of hedgehog readouts Gli1 and Ptch1 after darinaparsin treatment.

F: To determine whether darinparsin affects the expression of hedgehog effectors Gli1 and Gli2 darinaparsin was given daily (50mg/kg) to Gli1-nLacZ, Gli2-nLacZ reporter mice (mixed background of S129, Swiss Webster and C57Bl/6J; n=3 each, 2 males each, 8-10 week old,) starting 2 days prior to UUO. Mice were sacrificed at day 10 after surgery. 5-bromo-4-chloro-3-indolyl-β-D-galactopyranoside (X-gal) staining of these reporter mice shows a reduced number of Gli1 and Gli2 expressing cells. *p<0.05, ***p<0.001 vs vehicle treated mice by t-test, data is presented as mean±SEM, all scale bars 50µm

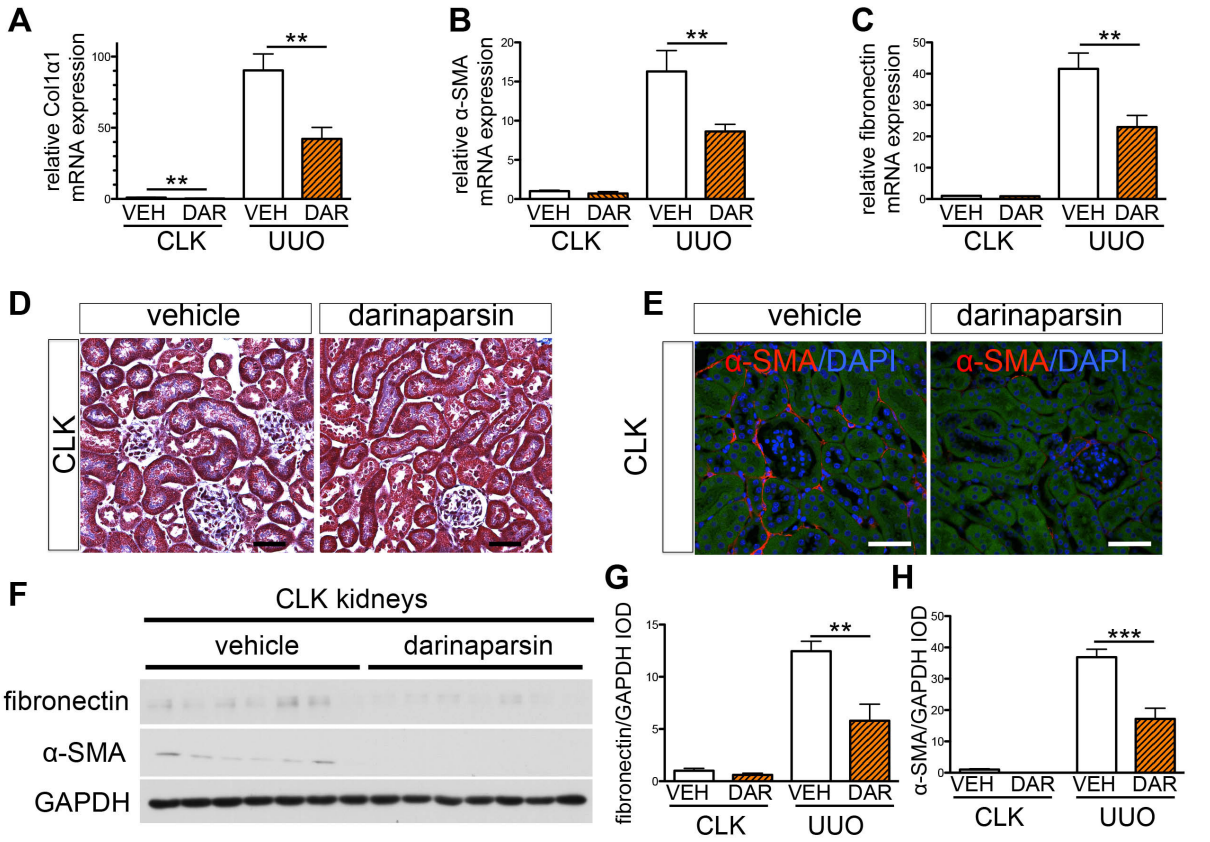

Figure S11: Darinaparsin treatment reduces mRNA expression of fibrotic readouts following unilateral ureteral obstruction (UUO)

Wildtype mice (C57Bl/6J, 8-10 weeks of age, all males) were subjected to UUO surgery and treated with darinaparsin (DAR, n=9) or vehicle (VEH, n=7) starting 2 days prior to UUO surgery until day 10. (Experiment of figure 5)

A-C: CollagenIαI, fibronectin and alpha smooth muscle actin (α-SMA) mRNA expression in whole unilateral ureteral obstruction (UUO) and contralateral (CLK) kidneys.

D-E: Representative images of trichrome stained or α-SMA immunostained contralateral non-injured kidneys (CLK).

F: Western blot for fibronectin and α-SMA from whole CLK kidneys.

G-H: Western blots for fibronectin and α-SMA were quantified by integrated optical density (IOD) indicating a significant reduced expression of both proteins in day 10 UUO kidneys from mice treated with darinaparsin (DAR) compared to the vehicle (VEH) group. (Representative western blot from UUO kidneys is shown in figure 5G).

**p<0.01, ***p<0.001 vs vehicle treated mice by t-test, data is presented as mean±SEM, all scale bars 50µm

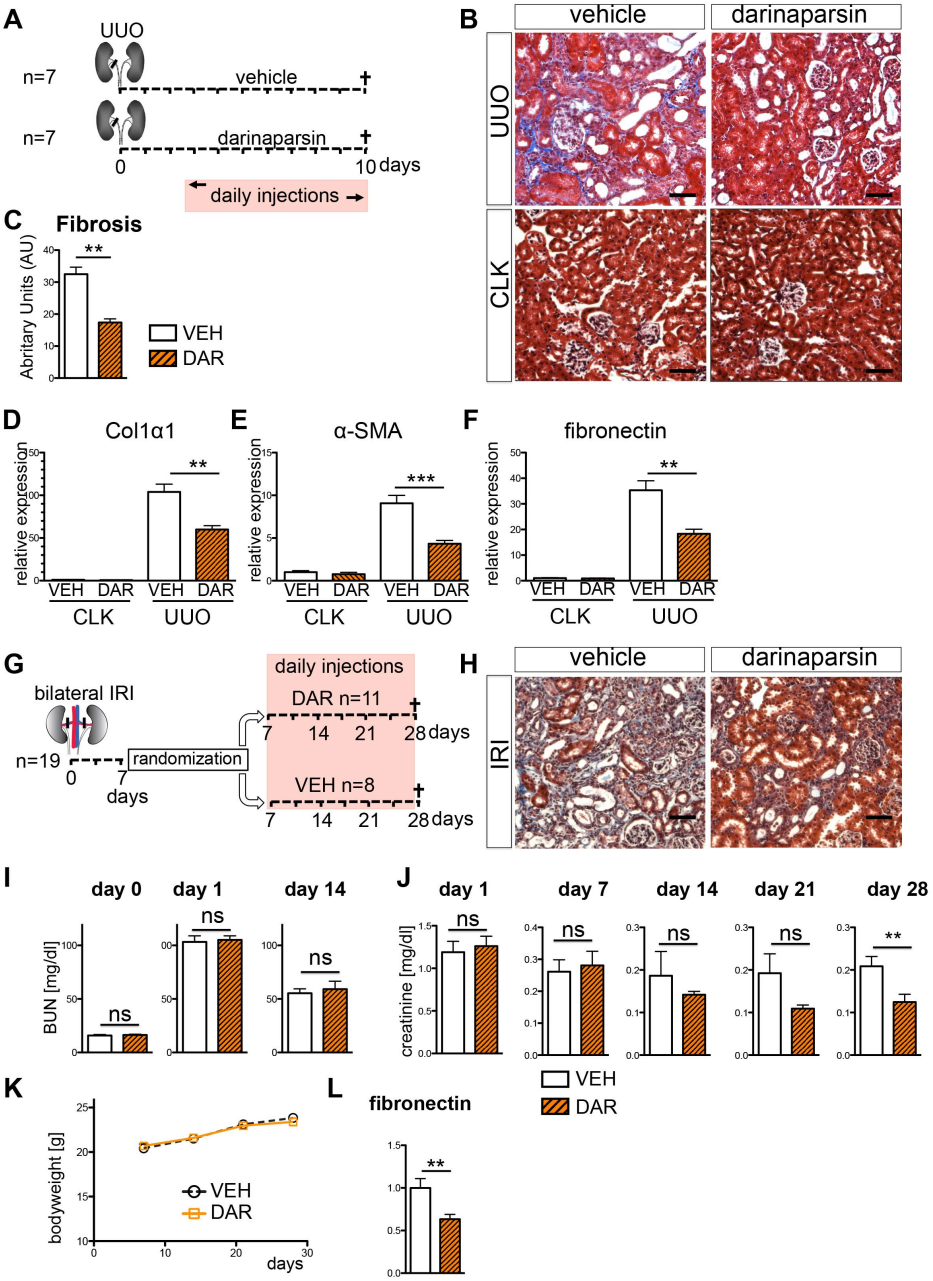

Figure S12: Therapeutic effect of darinaparsin after unilateral ureteral obstruction and bilateral ischemia re-perfusion injury.

A-F: A total of 14 mice (C57Bl/6J, 8-10 weeks old, all males) underwent unilateral ureteral obstruction (UUO), starting 2 days after surgery until sacrification 10 days after surgery n=7 mice were treated daily with darinaparsin (DAR, 50mg/kg i.p.) whereas n=7 mice served as a control group (daily injections of vehicle, VEH, i.p.) (A). Staining for Masson´s trichrome (B) and scoring revealed significant less interstitial fibrosis in the UUO kidneys of darinaparsin treated mice when compare to the UUO kidney of the control group (C). Determination of mRNA expression by quantitative realtime PCR demonstrated a significant lower expression of the fibrotic readouts collagen-1-alpha-1 (Col1α1, D), (alpha smooth muscle actin (α-SMA, E) and fibronectin (F) in the unilateral UUO kidneys of darinaparsin treated animals compared to vehicle treated animals.

G-H: Scheme of the bilateral ischemia re-perfusion injury experiment in n=19 wiltype mice (C57Bl/6J, 8-10 weeks old, all males) (G), representative Masson´s trichrome stained sections of IRI kidneys (H).

I: Measurement of blood urea nitrogen (BUN) revealed no significant difference between both groups at baseline and 7 days after ischemia reperfusion injury and at day 7 of treatment.

J: Measurement of serum creatinine indicated no significant difference between both groups at baseline and randomization with a significant lower creatinine in the darinaparsin treated group at 28 days after ischemia reperfusion injury.

K: Bodyweight data over time for vehicle (VEH) and darinaparsin (DAR) treated mice after ischemia reperfusion injury.

L: Quantitative realtime PCR analysis demonstrated significant lower mRNA expression of fibronectin in the IRI kidneys of darinaparsin treated mice. *p<0.05, **p<0.01, ***p<0.001, by t-test, data is presented as mean±SEM, all scale bars 50µm.

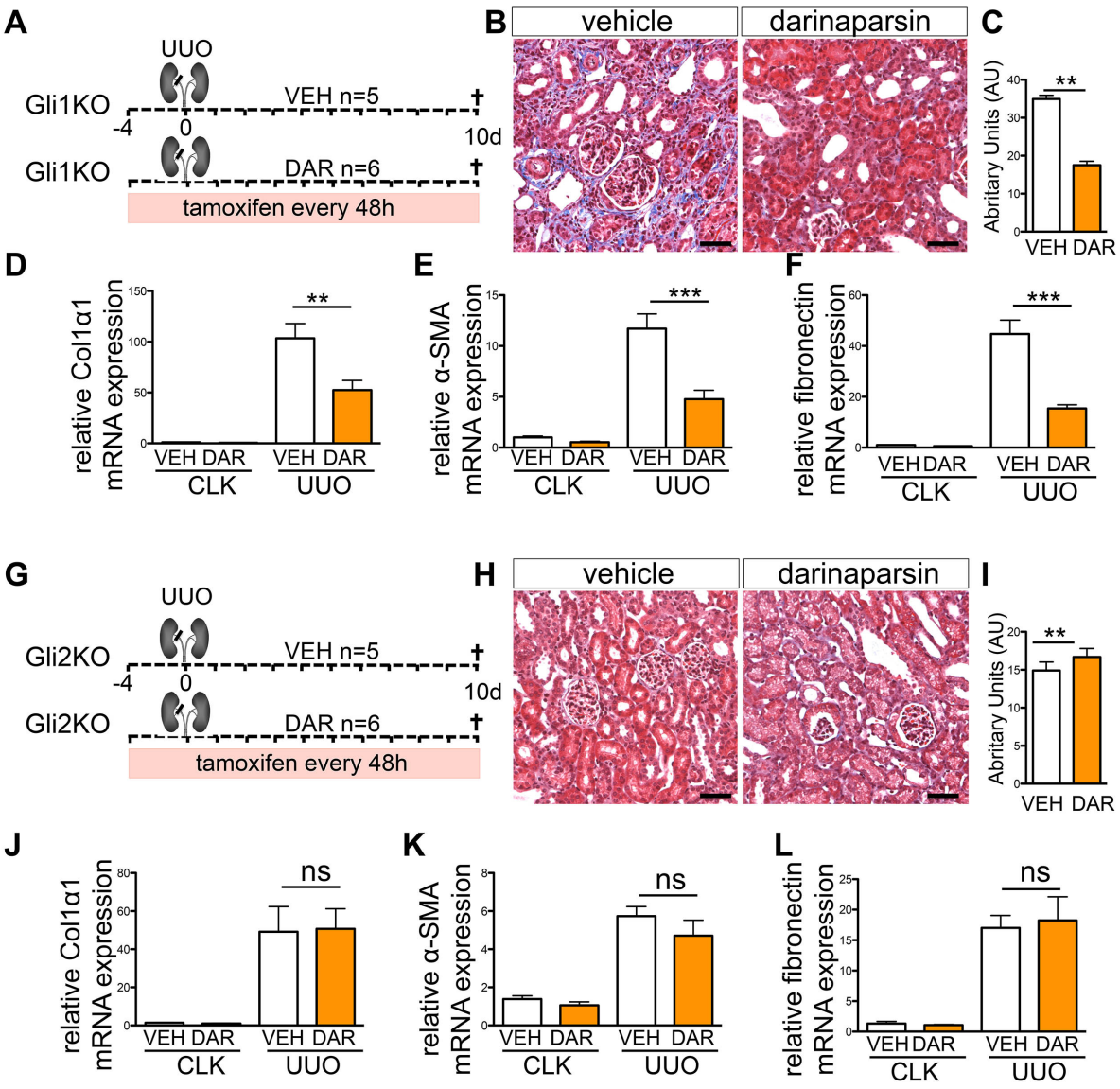

Figure S13: Darinaparsin treatment ameliorates fibrosis in Gli1KO mice but has not appreciable effect in conditional Gli2 knockout mice.

A: Gli1KO mice (Gli1LacZ$^{+/+}$; mixed background of 129S, Swiss Webster and C57Bl/6J, 8-10 weeks old) underwent unilateral ureteral obstruction (UUO) surgery and were treated with darinaparsin (DAR, n=6, 3 males, 50mg/kg bodyweight) or vehicle (normal saline, VEH n=5, 3 males) daily starting 2 days prior to surgery until euthanasia (day 10 after surgery). Mice of both groups received tamoxifen (10mg, p.o.) every 48h starting 2 days prior to UUO surgery.

B-C: Representative trichrome stained images and quantification of interstitial fibrosis indicating significantly decreased fibrosis in Gli1KO mice treated with darinaparsin compared to the vehicle treated group.

D-F: Quantitative realtime PCR for fibrotic readouts collagenIαI (ColIαI), alpha smooth muscle actin (α-SMA) and fibronectin demonstrates reduced mRNA expression in the darinaparsin (DAR) treated group compared to the vehicle (VEH) treatment group of Gli1KO mice.

G: Gli2KO mice (Gli1CreER$^{+/-}$;Gli2flox$^{+/+}$; mixed background of 129S and C57Bl/6J, 8-10 weeks old) underwent UUO surgery and were treated with darinaparsin (DAR, n=6, 3 males) or vehicle (VEH, n=5, 3 males) starting 2 days prior to surgery until 10 days after surgery. Mice received tamoxifen (10mg, p.o.) every 48h starting 2 days prior to surgery until euthanasia.

H-I: Representative trichrome stained sections and quantification of interstitial fibrosis indicating no difference between the darinaparsin and vehicle treated group of Gli2KO mice.

J-L: Quantitative realtime PCR for fibrotic readouts collagenIαI (ColIαI), alpha smooth muscle actin (α-SMA) and fibronectin from whole kidneys of Gli2KO mice treated with darinaparsin (DAR) or vehicle (VEH). **p<0.01, ***p<0.001, by t-test, data is presented as mean±SEM, all scale bars 50µm.

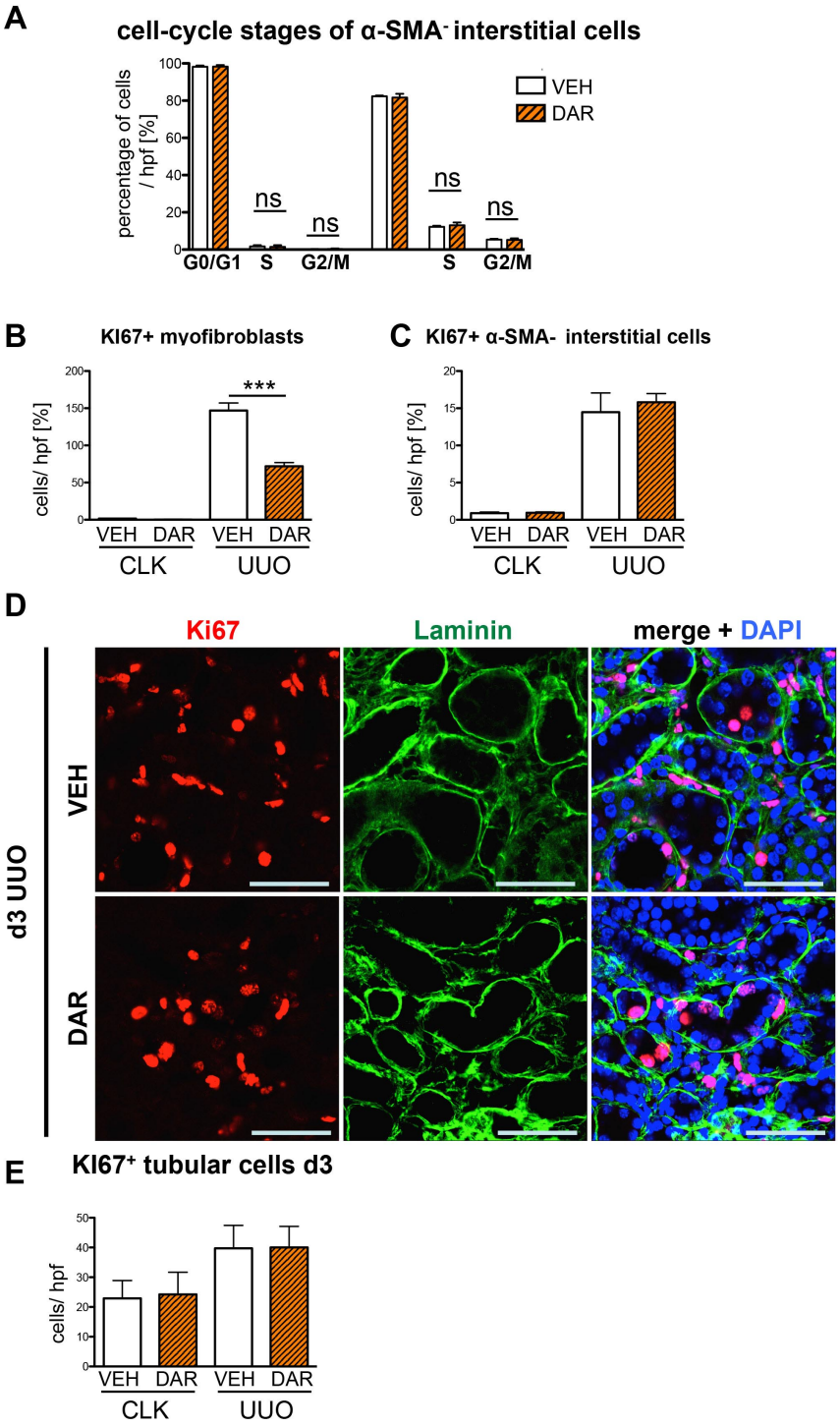

Figure S14: Darinaparsin treatment reduces proliferation of interstitial myofibroblasts but does not affect proliferation of other renal cell-types at day 3 following UUO.
Wildtype mice (C57Bl/6J, 8-10 weeks old, all males) were treated with darinaparsin (50mg/kg, n=6) or vehicle (n=6) starting 2 days prior to unilatereal ureteral obstruction (UUO) surgery and sacrified at day 3 after surgery. Bromdesoxyuridin (BrDU) was injected (100mg/kg) 3 hours prior to sacrification.
A: Cell cycle stages for interstitial non-myofibroblast cells (αSMA-) do not differ between darinaparsin (DAR) or vehicle (VEH) treated mice 3 days after UUO surgery.
B: Quantification of Ki67+ interstitial αSMA+ cells indicates reduced proliferation of myofibroblasts in the UUO kidneys of darinaparsin treated mice 3 days after surgery.
C: Quantification of Ki67+ interstitial αSMA- cells (non myofibroblasts) indicates no difference between darinaparsin and vehicle treated group.
D-E: Laminin staining was performed to delineate the tubules and cycling tubular epithelial cells were identified by staining for Ki67 and counting of Ki67+ cells within tubules (surrounded by laminin + basement membrane). ns=non-significant by one way ANOVA with posthoc Bonferroni; ***p<0.001, by t-test, data is presented as mean±SEM, all scale bars 50μm.

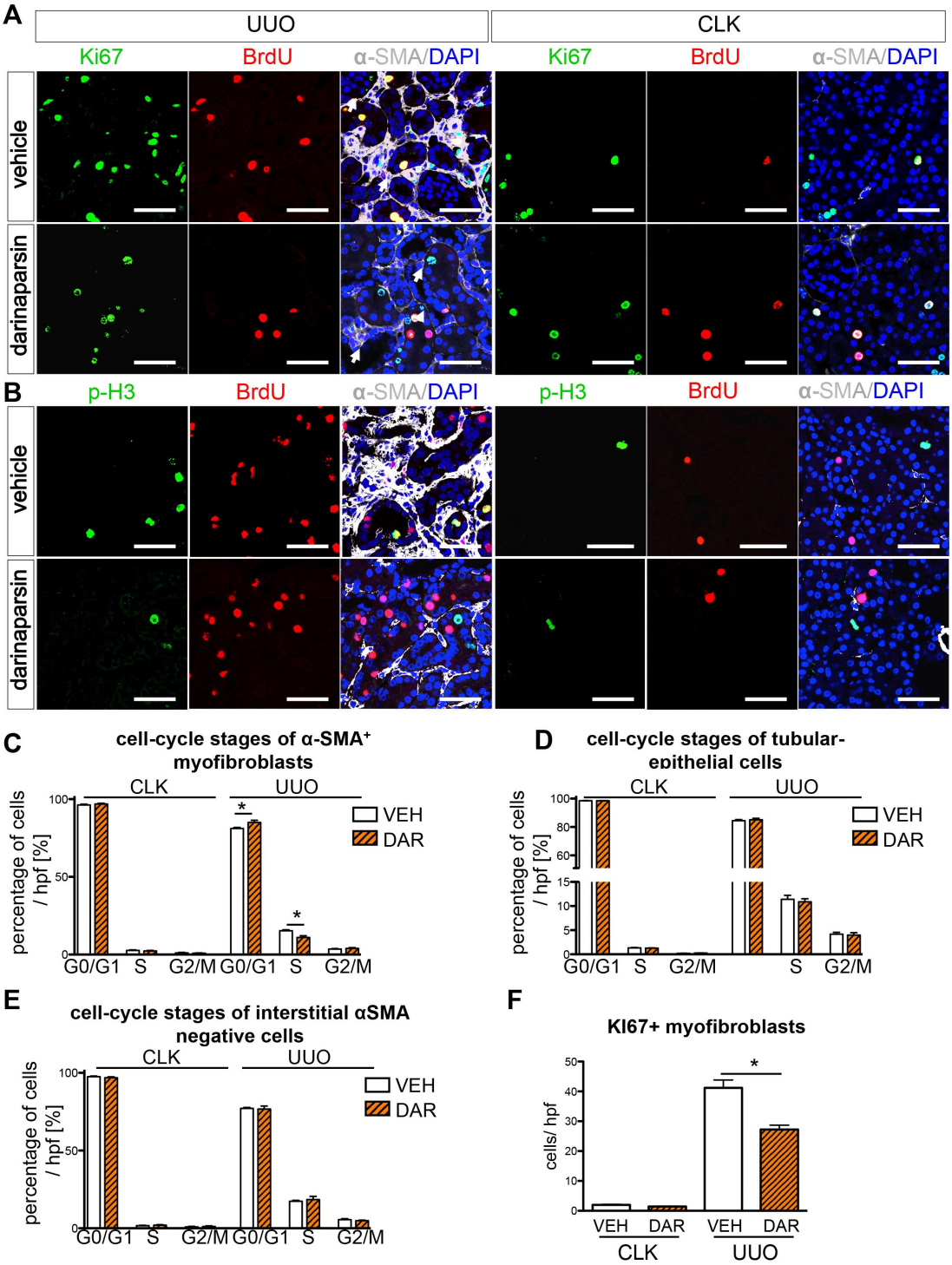

Figure S15: Darinaparsin treatment reduces proliferation of interstitial myofibroblasts 10 days after UUO surgery while tubular-epithelial cells and interstitial non-myofibroblasts were not affected.
Wildtype mice (C57Bl/6J, 8-10 weeks old, all males) underwent unilateral uretereal obstruction (UUO) surgery and received darinaparsin (DAR, n=7) or vehicle (VEH, n=7) daily starting 2 days after surgery until euthanasia at 10 days after surgery. Mice were injected with BrdU 3 hours prior to euthanasia.
A-B: Representative images of costained kidney sections from UUO and non-injured contralateral kidneys (CLK). Costaining for Ki67 + BrdU + alpha smooth muscle actin (αSMA) in A and phopspho-histone H3 (pH3) + BrdU + alpha smooth muscle actin (αSMA) in B.
C-E: Determination of cell-cycle stages indicated a G0/G1 cell-cycle arrest of interstitial myofibroblasts with no effect on tubular-epithelial cells or interstitial αSMA- cells (non-myofibroblasts) at day 10 UUO. Cell cycle stages for interstitial myofibroblasts (αSMA+), for interstitial non-myofibroblasts (αSMA-) and tubular epithelial cells were calculated as follows: s-phase= BrdU+ cells; G2/M-phase= pH3+ cells; G0/G1-phase= all cells – BrdU+ - ph3+.
F: Ki67+ interstitial myofibroblasts were quantified by counting of Ki67/αSMA double positive interstitial cells.
*p<0.05 by one way ANOVA with posthoc Bonferroni, data is presented as mean±SEM, all scale bars 50µm.

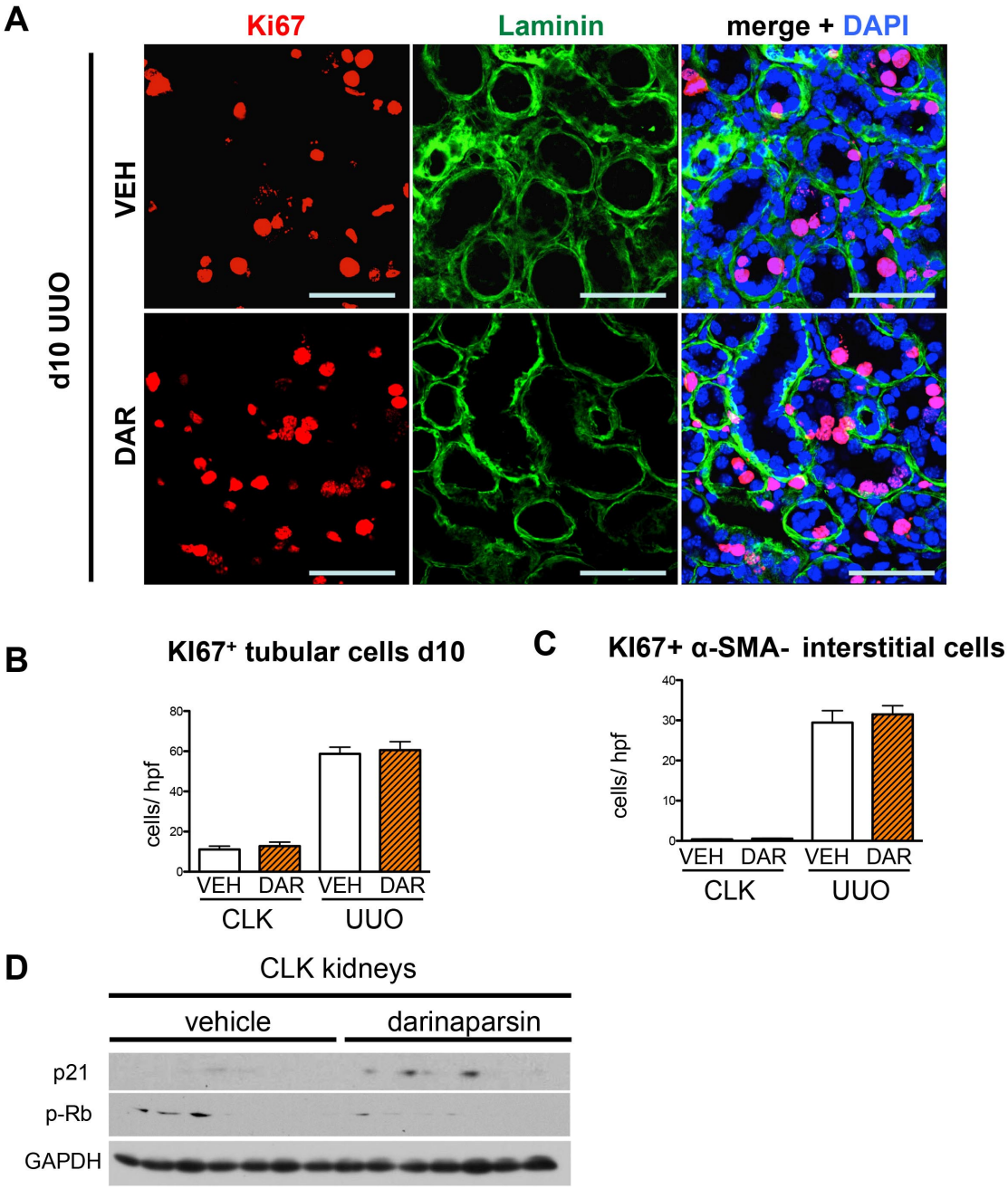

Figure S16: Darinaparsin treatment does not affect tubular epithelial proliferation at 10 days after UUO
A: Representative picture of kidney sections from day 10 UUO kidneys stained for Ki67 and laminin to determine tubular epithelial cell proliferation. Wildtype mice (C57Bl/6J, 8-10 weeks old, all males) received darinaparsin (DAR, n=7) or vehicle (VEH, n=7) daily from day 2-10 after UUO surgery.
B-C: We detected no difference in tubular epithelial Ki67+ cells (B) or cycling interstitial non-myofiroblasts (Ki67+/αSMA-) between the darinaparsin or the vehicle treated group-
D: Western blot analysis of whole CLK kidneys shows slightly increased levels of p21 with also a tendency to faintly reduction of phosphorylated retinoblastoma (p-Rb) in the darinaparsin treated mice. **(**UUO kidneys are shown in figure 6) Data is presented as mean±SEM, all scale bars 50µm.

Supplementary Table 1:

Primer pairs used for qt-RT-PCR in mouse:

Gene	Sequence
GAPDH	Fw 5′-AGGTCGGTGTGAACGGATTTG -3′
	Rv 5`-TGTAGACCATGTAGTTGAGGTCA -3′
Gli1	Fw5′- ATCACCTGTTGGGGATGCTGGAT-3′
	Rv5′- CGTGAATAGGACTTCCGACAG -3′
Gli2	Fw5′-GTTCCAAGGCCTACTCTCGCCTG -3′
	Rv5′- CTTGAGCAGTGGAGCACGGACAT-3′
Ptch1	Fw5′- GCTGGAGGAGAACAAGCAAC-3′
	Rv5′- GAGCAAACATGTGCTCCAGA -3′
Col1α1	Fw5′- TGACTGGAAGAGCGGAGAGT-3′
	Rv5′-GTTCGGGCTGATGTACCAGT -3′
fibronectin	Fw5′-ATCTGGACCCCTCCTGATAGT -3′
	Rv5′-GCCCAGTGATTTCAGCAAAGG-3′
α-SMA	Fw5′-CTGACAGAGGCACCACTGAA -3′
	Rv5′- CATCTCCAGAGTCCAGCACA-3′

Supplementary Table 2:

Primer pairs used for qt-RT-PCR in human:

Gene	Sequence
GAPDH	Fw 5′- GACAGTCAGCCGCATCTTCT-3′
	Rv 5`- GCGCCCAATACGACCAAATC-3′
Gli1	Fw5′- GAGCCAGAAGTTGGGACCTC-3′
	Rv5′- CCTCGCTCCATAAGGCTCAG -3′
Gli2	Fw5′- AAAGGCCTCTCCTTTGGTGG-3′
	Rv5′- CTTCCTTCCTGGTGTCGCAT -3′
Ptch1	Fw5′- CTTCTGGGAAGGGGCGAAAT -3′
	Rv5′- AGCATTTCCTCCCAGCTGTC -3′
Col1α1	Fw5′- CCCAGCCACAAAGAGTCTACA-3′
	Rv5′- ATTGGTGGGATGTCTTCGTCT -3′
fibronectin	Fw5′-AACAAACACTAATGTTAATTGCCCA-3′
	Rv5′-TCGGGAATCTTCTCTGTCAGC-3′
α-SMA	Fw5′- ACTGCCTTGGTGTGTGACAA-3′
	Rv5′- CACCATCACCCCCTGATGTC-3′

Supplementary Table 3: Basic characteristic of patients included

Subject	Age / sex / race	Surgery (nephrectomy)	Indication/ pathology	Pre-operative SCr, mg/dL*	Interstitial fibrosis	Risk factors for CKD
1	51 / M / C	Radical	Papillary urothelial carcinoma	1.18	>90%	unilateral severe hydronephrosis, HTN
2	64 / M / C	Partial	RCC	1.09	<10%	HTN
3	63 / M / C	Partial	RCC	0.98	80%	HTN, gout
4	69 / F / A	Radical	Papillary urothelial carcinoma; hydronephrosis	0.88	>90%	HTN, Hyperlipidemia, DM
5	59 / M / C	Radical	RCC	0.86	20%	Gout
6	60 / M / C	Radical	RCC	1.40 (eGFR 52)	<10%	none
7	72 / M / C	Radical	RCC	1.42 (eGFR 49)	40%	CAD, DM, HTN
8	52 / M / C	Radical	RCC	1.00	<10%	HTN, Hyperlipidemia
9	50 / M / C	Partial	RCC	0.65	<10%	none
10	56 / F /C	Radical	Metanephric adenoma	0.90	<10%	none

Abbreviations: A, Asian; C, Caucasian; eGFR, estimated glomerular filtration rate, ml/min/1.73m^2; M, male; RCC, renal cell carcinoma; SCr, serum creatinine; CKD, chronic kidney disease; HTN, hypertension; CAD, coronary artery disease; DM, diabetes mellitus

* All eGFR > 60 unless noted